SLAC-PUB-10477

BaBar Forward Endcap Upgrade

F. Anulli [a], R. Baldini [a] A. Calcaterra [a], L. Daniello [a]
R. de Sangro [a]. G. Finocchiaro [a], P. Patteri [a], M. Piccolo [a],
M. Santoni [a], A. Zallo [a], C.H. Cheng [b], D.J. Lange [b],
D.M. Wright [b], R. Boyce [c], J, Krebs [c], R. Messner [c],
G. Putallaz [c], W.J. Wisniewski [c], A. Buzzo [d], G. Crosetti [d],
M. LoVetere [d], S. Minutoli [d], S. Passaggio [d], P. Pollovio [d],
E. Robutti [d], S. Tosi [d], A. Trovato [d], C. Cartaro [e], F. Fabozzi [e],
L.Lista [e], D. Piccolo [e], P. Paolucci [e], C. Avanzini [f],
M. Carpinelli [f], F. Forti [f], N. Neri [f], E. Paoloni [f], D. Rizzi [f],
F. Bellini [g], A. Buccheri [g], G. Cavoto [g], D. del Re [g], R. Faccini [g],
F. Ferrarotto [g], F. Ferroni *,[g] C. Gargiulo [g], M. Gaspero [g],
R. Lunadei [g], M.A. Mazzoni [g], S. Morganti [g], A. Pelosi [g],
M. Pierini [g], G. Piredda [g], C. Voena [g], N. Sinev [h], D. Strom [h],
S. Foulkes [i], K. Wang [i], H. R. Band [j], J. Hollar [j], P. Tan [j],

[a] *Laboratori Nazionali di Frascati, INFN, Italy*

[b] *Lawrence Livermore National Laboratory, USA*

[c] *Stanford Linear Accelerator Center, Menlo Park, CA, USA*

[d] *Università di Genova & INFN Sezione di Genova, Italy*

[e] *Università di Napoli "Federico II" & INFN Sezione di Napoli, Italy*

[f] *Università di Pisa & INFN Sezione di Pisa, Italy*

[g] *Università di Roma "La Sapienza" & INFN Sezione di Roma, Italy*

[h] *University of Oregon, Eugene, OR, USA*

[i] *University of California, Riverside, CA, USA*

[j] *University of Wisconsin, Madison, WI, USA*

Abstract

The muon and neutral hadron detector (Instrumented Flux Return or IFR) in the forward endcap of the BaBar detector at SLAC was upgraded by the installation of a new generation of Resistive Plate Chambers (RPCs) and by increasing the absorber. The chamber replacement was made necessary by the rapid aging and efficiency loss of the original BaBar RPCs. Based on our experience with those original RPCs and 24 RPCs with thinner linseed oil treatments, improvements in

* *Work supported in part by the Department of Energy Contract DE-AC03-76SF00515*

the design, construction, and testing of the new generation RPCs were implemented and are described in detail.

Key words: RPC, Muon detection
PACS: 29.40.C

1 Introduction

The BaBar detector [1] has operated over 2000 m^2 of Resistive Plates Chambers (RPC [2]) as muon and neutral hadron detectors (Instrumented Flux Return) since 1999. BaBar RPCs operate at 6700-7600 Volts in limited streamer mode, using a gas mixture of 4.4% isobutane, 60% argon and 35.6% freon 134a. The BaBar IFR is currently the largest RPC system in operation which uses bakelite and linseed oil in its construction. Details of the original BaBar RPC production (manufactured by General Tecnica [3] in 1996-7) can be found in Reference [1].

Most of the original RPCs have lost efficiency and many are now completely inefficient [4]. Both the linseed oil used to coat the inner bakelite surfaces and the graphite coating on the outer surfaces are implicated as contributors to the efficiency loss which was accelerated by the operation of the RPCs at temperatures $29 - 34^oC$ during the first summer of colliding beam data [1]. After installation of water cooling of the BABAR steel in fall 1999, temperatures remained stable at $19 - 22^oC$ in the barrel and $21 - 24^oC$ in the endcaps. However, RPC efficiencies continued to decline as seen in Fig. 1 where the average RPC efficiencies in the barrel and endcaps are plotted. The average RPC efficiency in the barrel fell below 50% in 2002. Since there are 19 RPC layers in the barrel, the muon identification algorithm is relatively insensitive to the loss of a single RPC. The cumulative effect of the RPC losses has dropped the muon identification efficiency from 87% to 78% in the barrel at a pion misidentification rate of 4%. If the trend continues as expected all muon identification capability would be lost.

Despite an intensive program of RPC studies [5], no permanent reversal of the efficiency losses has been achieved. Replacement was the only viable option. To test if changes to the coating would eliminate the observed RPC problems 24 new RPCs were built and installed in the forward endcap in fall of 2000. Some of the replaced chambers were studied in test stands and nearly all of them showed problems with the linseed oil coating. The new chambers were

* Corresponding author
Email address: fernando.ferroni@roma1.infn.it (F. Ferroni).

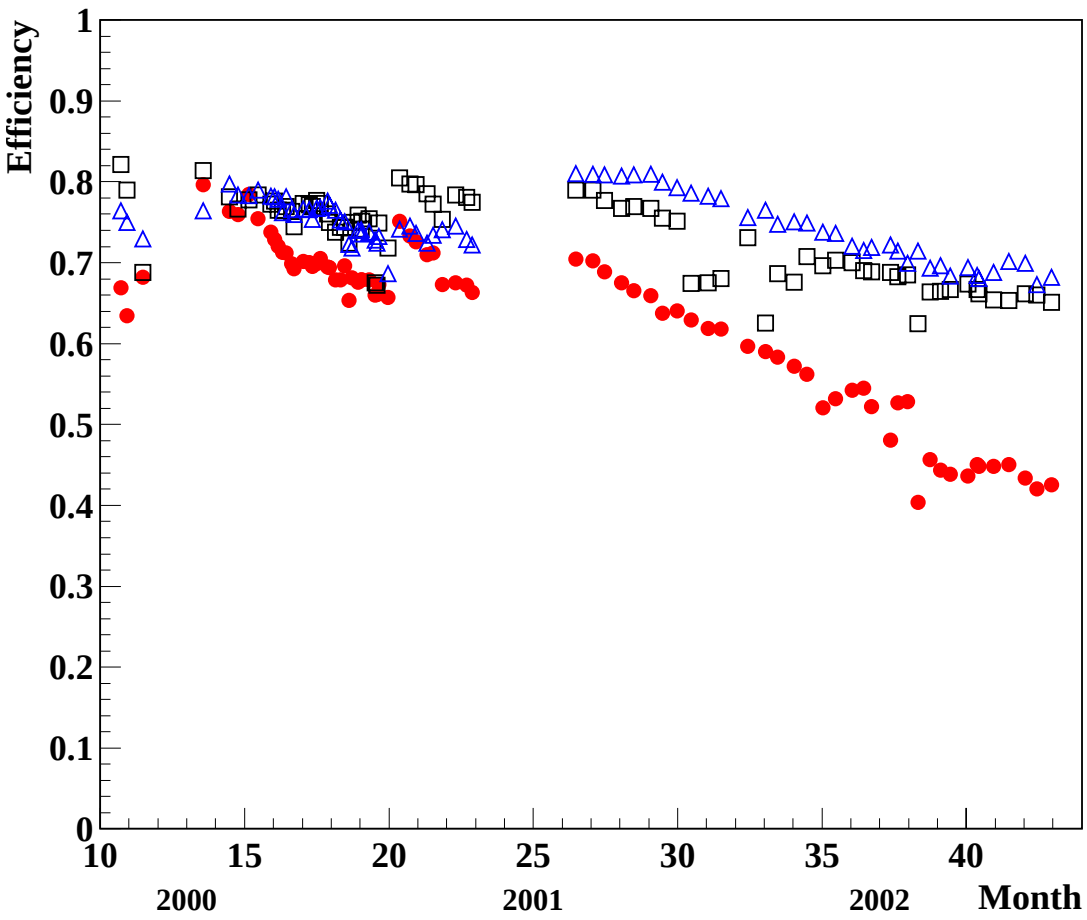

Fig. 1. The average RPC efficiency in the barrel (circles), forward end cap (triangles) and backward end cap (squares) are shown as a function of time until the summer of 2002. The efficiency is evaluated using $\mu^+\mu^-$ pairs from collision data.

built with the same techniques as the original production except that a new oiling technique developed by the RPC community was used. The change in oiling technique was suggested by the much smoother bakelite available at the time. The linseed oil layer obtained was approximately 3 times thinner than before and was well cured. The average efficiency of 16 of these new RPC is shown in Fig. 2 for 2001-2. Also plotted for 2002-3 are the efficiencies of the 4 RPCs from the 2000 production that remain in the endcap. The initial performance of these chambers was encouraging, showing an average efficiency decrease of less than 2% in the first year and about 6% in 3 years.

Replacement of the Barrel RPCs is a difficult engineering task and would require over 6 months to install. By contrast, replacement of chambers in the open geometry of either end cap was feasible by extending the normal summer shutdown from 8 to 10 weeks. BaBar is an asymmetric detector with 49% of the solid angle acceptance in the center of mass covered by the forward endcap. The choice was therefore made to replace the forward endcap RPCs as a test of the new RPC performance and of installation methods.

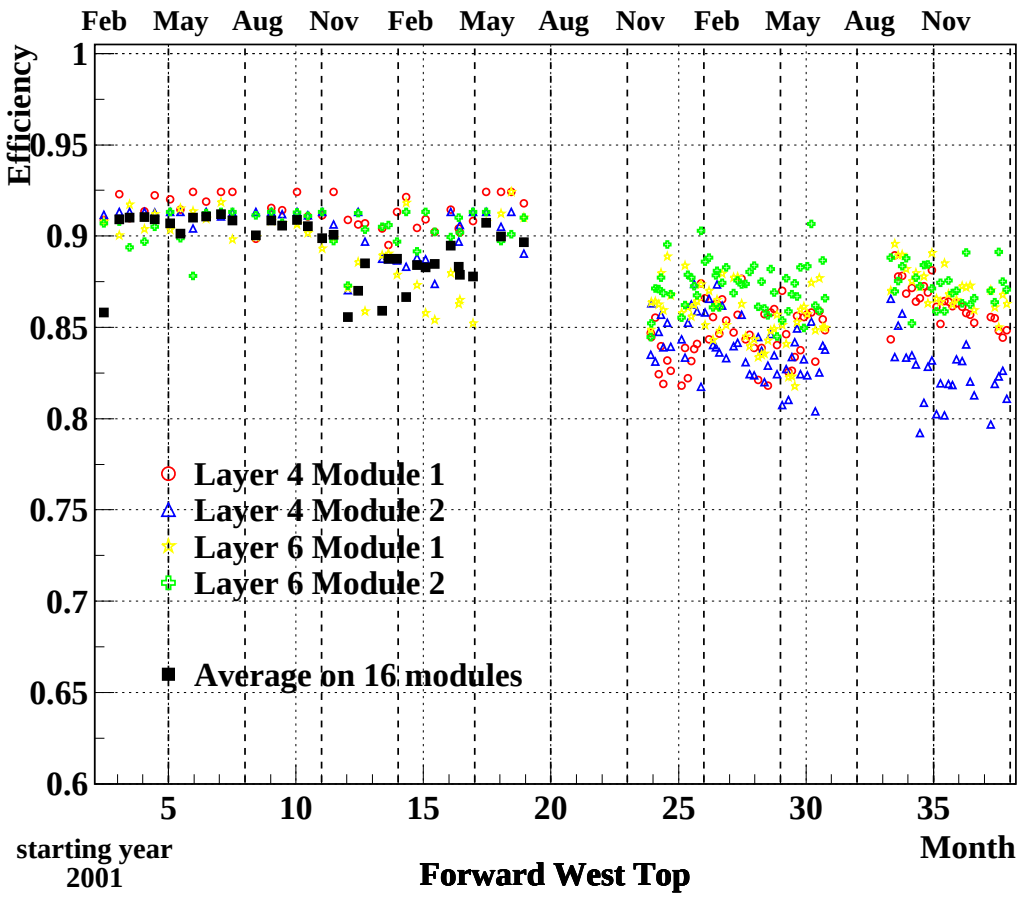

Fig. 2. Average Efficiency of the inner 24 RPCs (black squares) installed in the fall of 2000 versus time. All but four of these RPCs were replaced in the summer of 2002. The efficiency of the remaining four are plotted until early 2004.

2 Design

When it became clear that the RPCs would need to be replaced, the entire IFR system design was reappraised. The primary need was, of course, to build reliable and efficient RPCs. However, other design modifications such as adding more absorber or changing the distribution of the detector planes which could improve the system performance and reliability were investigated. Another consideration was to make the outer layers of the system less sensitive to failures of single RPC modules by putting two detector planes in each layer. Finally, other parts of the IFR infrastructure, the high voltage and gas distribution systems, had proven difficult to operate, adjust, and maintain, and could also be improved. The present note concentrates on the overall absorber design, RPC production and testing. A follow-up note will describe the upgraded gas distribution and monitoring system.

2.1 IFR overview

The Instrumented Flux Return (IFR) was designed to identify muons with high efficiency and good purity, and to detect neutral hadrons (K_L^0 and neutrons) over a wide range of momenta and angles. Muons are important for tagging the flavor of neutral B mesons and for reconstruction of the J/ψ . K_L^0 detection allows the study of CP eigenstates such as $B \to J/\psi K_L^0$. These two requirements conflict at some level since optimal muon identification calls for a large amount of absorber to filter out pions while the neutral hadron measurements require fine absorber segmentation. The total radius of the detector was dictated by external constraints, so a design compromise was necessary. The BaBar steel is segmented into 19 (barrel) or 18 (endcap) plates, increasing in thickness from 2 cm for the inner plates to 10 cm for the outermost plate. Single gap RPC planes were inserted into the 3.2-3.5 cm gaps between plates for a total of 19 RPC layers in the barrel and 18 in the endcaps. The total iron thickness for a penetrating track was 65 cm in the barrel and 60 cm in the endcaps. Adding the electro-magnetic calorimeter material ($\simeq$ 1 nuclear interaction length (λ)) brought the total absorbing power to 5.4λ for a particle impinging at a polar angle of 31^o.

The observed performance of the muon identification system [1] has been tested on samples of muons mostly from $\mu\mu\gamma$ final states and pions from three-prong τ decays and $K_S \to \pi^+\pi^-$ decays. A muon detection efficiency of close to 90% has been was achieved in 2000 in the momentum range of $1.5 < p < 3.0$ GeV/c while keeping the rate of pion misidentification at $\approx 8\%$. The hadron misidentification can be reduced by a factor of about two by a tighter selection criteria which lowers the muon detection efficiency to about 80%. Much lower pion misidentification rates could be achieved if the absorber thickness is increased.

The longitudinal distribution of K_L candidates found within the IFR (see Fig. 3) shows that most are detected in the finely segmented inner layers. Less than 10% of detected K_L's interact in the last 8 layers.

2.2 Detector upgrade

The detector performance described above suggested that a different ratio between absorber plates and active counters could deliver better μ/π separation without significantly diminishing the number of detected K_L. The first step was to optimize the absorber and detector design for tracks traversing the entire endcap. Extensive MonteCarlo studies [6] were performed with different numbers of absorber and detection planes. The total weight of additional

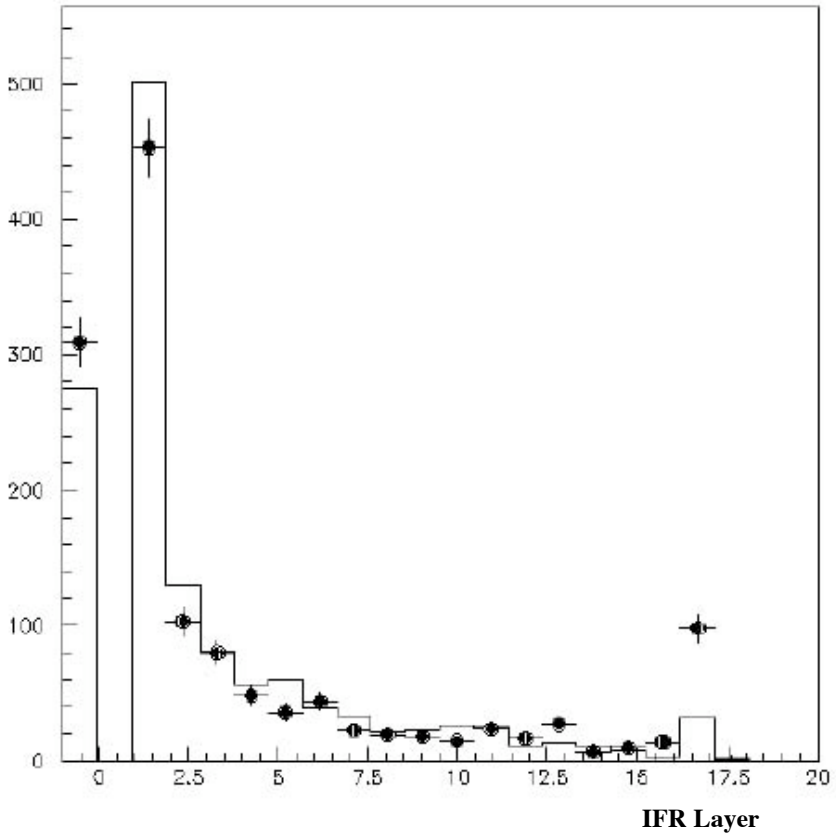

Fig. 3. First IFR layer hit by K_L candidates in $B \to J/\psi K_L^0$ decays. The histogram shows the MonteCarlo prediction and black dots data. The spike in the last layer is due to background noise in the outermost forward endcap layer. The K_L identification software requires that the first layer hit is before layer 14.

material was limited to 50 tons by earthquake safety considerations. As an example, we show the predicted performance of three different detector configurations in Fig. 4.

The simulations show that the pion misidentification rate was substantially reduced by adding absorber while preserving a high muon detection efficiency. A target value of better than 2% at 85% μ efficiency seemed reasonable and could be obtained by sacrificing a few active layers which, if chosen properly, would not spoil the K_L detection efficiency.

A second design concern was to improve the system robustness in the outer layers since most of the improved performance requires a fully efficient last layer. To provide redundancy, 2 single gap RPC chambers were placed in each of the last two steel gaps. These chambers have independent high voltage, gas, and data acquisition connections.

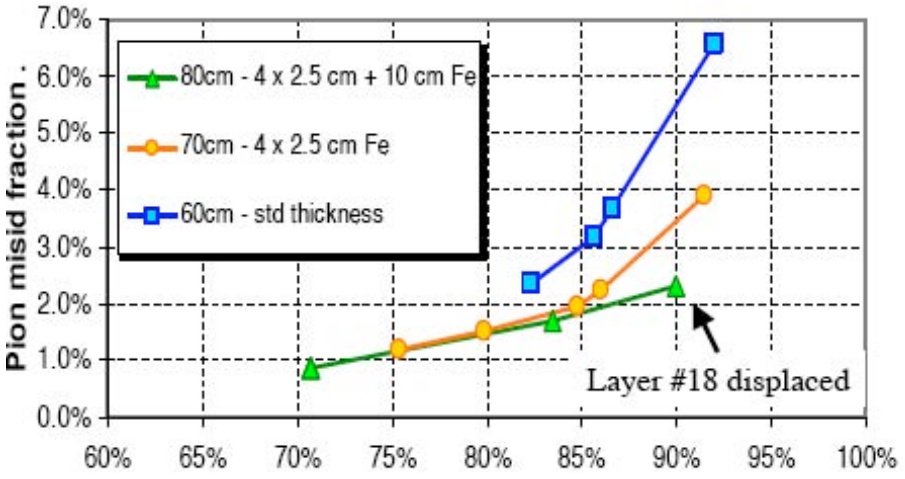

Fig. 4. The simulated detector response, muon identification efficiency versus pion misidentification for three designs of differing absorber thickness. Squares are the original BaBar detector. Circles are the original detector with 4 active layers replaced by brass. The triangular points have besides the latter modification another RPC plane added behind a slab of 10 cm of iron. In this study a single RPC layer is assumed to be 95% efficient.

The new geometry shown in Fig. 5 replaced five of the internal RPC layers with brass slabs 2.5 cm thick. The existing single plane of RPCs external to the endcap steel was removed and replaced by a double layer of RPCs, an additional 10 cm of steel, a second double layer of RPCs, and a final 2.5 cm steel plate. This geometry has two benefits: it increases the amount of absorber before the last detector layer from 5.4 to 7.3 λ and it has several detector planes at 5-6λ which are well shielded from backgrounds.

It was also necessary to improve muon identification for tracks traversing the overlap region between the barrel and endcap to match the new endcap. For polar angles between 45deg and 53deg , the existing steel thickness was 56-66 cm for a total of 5λ. By adding a double layer of RPCs outside the existing steel flux return bars the amount of absorber before the last detector plane would increase to 7.5λ. A belt layer of two RPCs surround all sides of the End Cap except the bottom were installation would have been impossible.

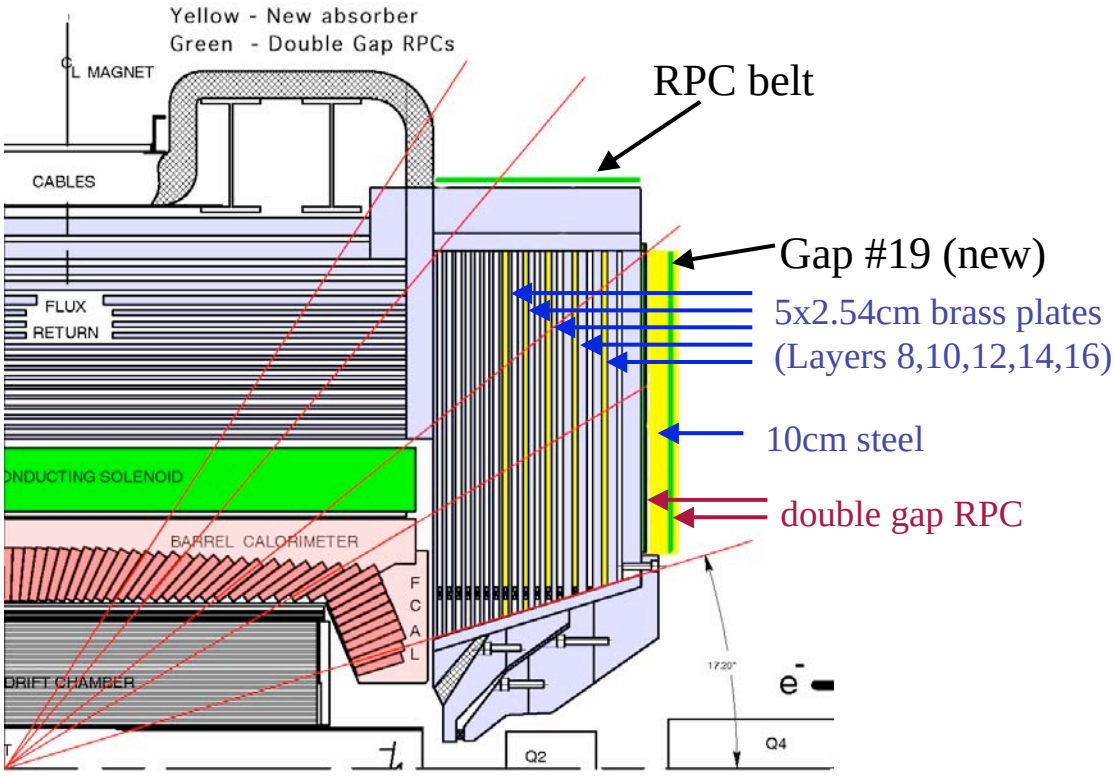

Fig. 5. The design of the new Forward End Cap.

3 Resistive Plate Counters

The original production of BaBar RPCs exhibited several failure modes. Changes in RPC behavior were initially characterized by non-reversible increases in the dark current (most but not all of the current increase with temperature was reversible). Next appeared inefficient regions in the RPC area, and shifts in the RPC high voltage plateau to higher voltages and lower plateau efficiencies. The increased currents and lowered efficiencies were reproduced in test stands by heating spare RPC modules to 36^o C for a week. An autopsy of these chambers showed large drops of liquid linseed oil spanning the gap between the HV planes. Such drops would reduce the local electric field and produce areas of lowered efficiency. Several forward endcap chambers were also found to contain excessive oil when removed in 2000, as shown in Fig. 6.

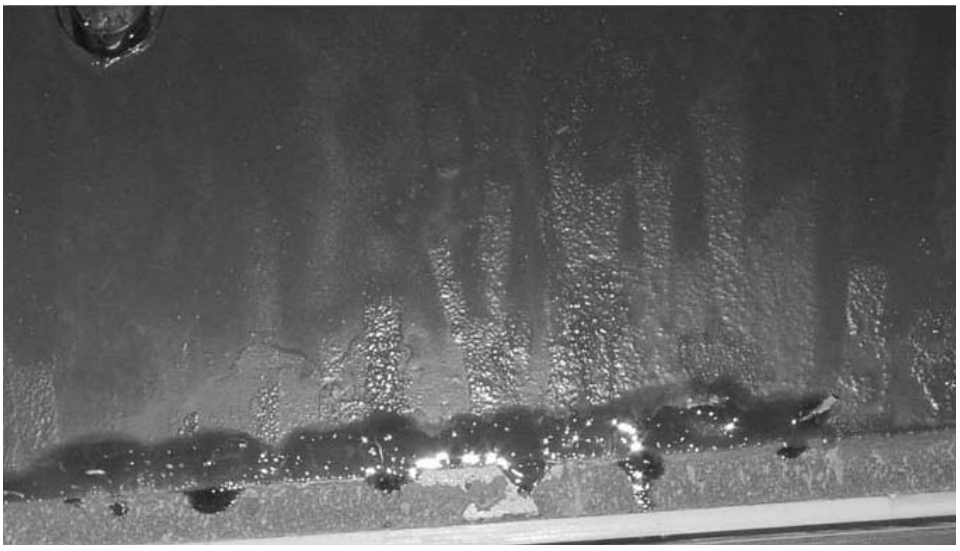

Fig. 6. A photograph of the lower inside edge of an endcap RPC removed from BaBar in 2000. The dark colored linseed oil collected on the bottom frame has a significantly lower resistivity than either fresh or cured linseed oil [9].

Oil from damaged RPCs and from spare RPC modules which were never used were analyzed by FTIR spectroscopy [8]. The spectroscopy saw evidence for fatty acids resulting from the decomposition of the linseed oil as well as phthalates. Phthalates, used as plasticizers in industry, could inhibit the proper curing of the linseed oil. The presence of the phthalates in the spare RPCs suggested that the linseed oil supply may have become contaminated, inhibiting the proper drying and polymerization of the linseed oil.

Twenty four RPCs were produced and installed into the forward endcap in the fall of 2000 to test new procedures for coating the bakelite with linseed oil. No other substantive changes were made. The surface of these chambers was hard and dry to the touch. Two similar RPCs were subjected to a one week heating test. Neither RPC lost efficiency, but one showed a large increase in singles rate and dark current. When opened, this RPC had few linseed oil drops and the bakelite surface was generally dry. However, there were bumps, discolored regions, and droplets clustered near the gas inlets. Further visual inspection showed that debris and impurities, probably produced by the machining of the gas connections, were located in that zone and were the source of local discharges (Fig. 7). Later autopsies of chambers which had been installed in the forward endcap showed similar problems.

Changes were clearly needed in the RPC production technique. Thin well-cured linseed oil layers are required. Thinner linseed oil layers make the chambers more sensitive to bakelite surface quality requiring a thorough revision of

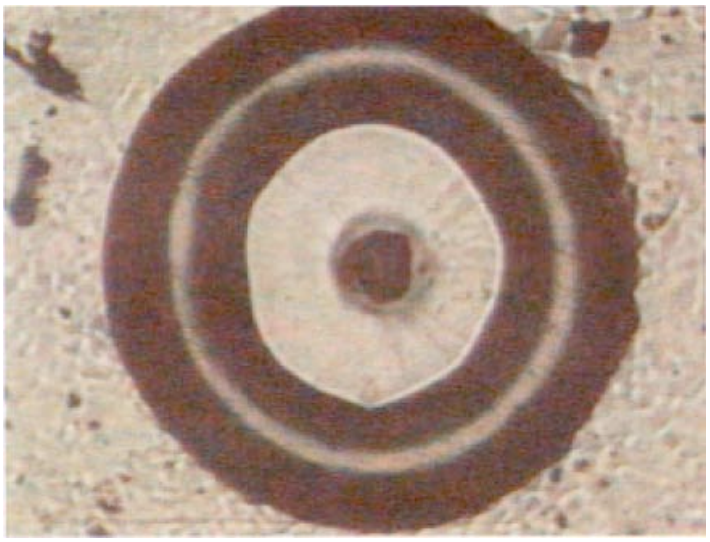

Fig. 7. Picture of a discharge region. The diameter of the damaged region (crater-like) is 1.2 mm.

the production process and quality control procedures.

3.1 Production

The new chambers have to fit inside the hexagonal shape of the end-cap. The endcap is split vertically into two doors. Each door is further divided into 3 sections: top, middle, and bottom. Since the top and bottom are identical except for a rotation only two basic shapes were needed as shown in Fig. 8. Each chamber consists of two separate high voltage modules which were connected in series to make a single gas volume. The belt chambers are of a simpler rectangular design.

The standard RPC production proceeds in several steps which are outlined below.

- Raw material procurement and preparation: measure bakelite resistivity and inspect surface quality; cut the bakelite to shape and clean surfaces; coat the outer bakelite with graphite and PET film; prepare linseed oil mixture.
- Gas volume assembly: glue spacers and frames under a vacuum press.

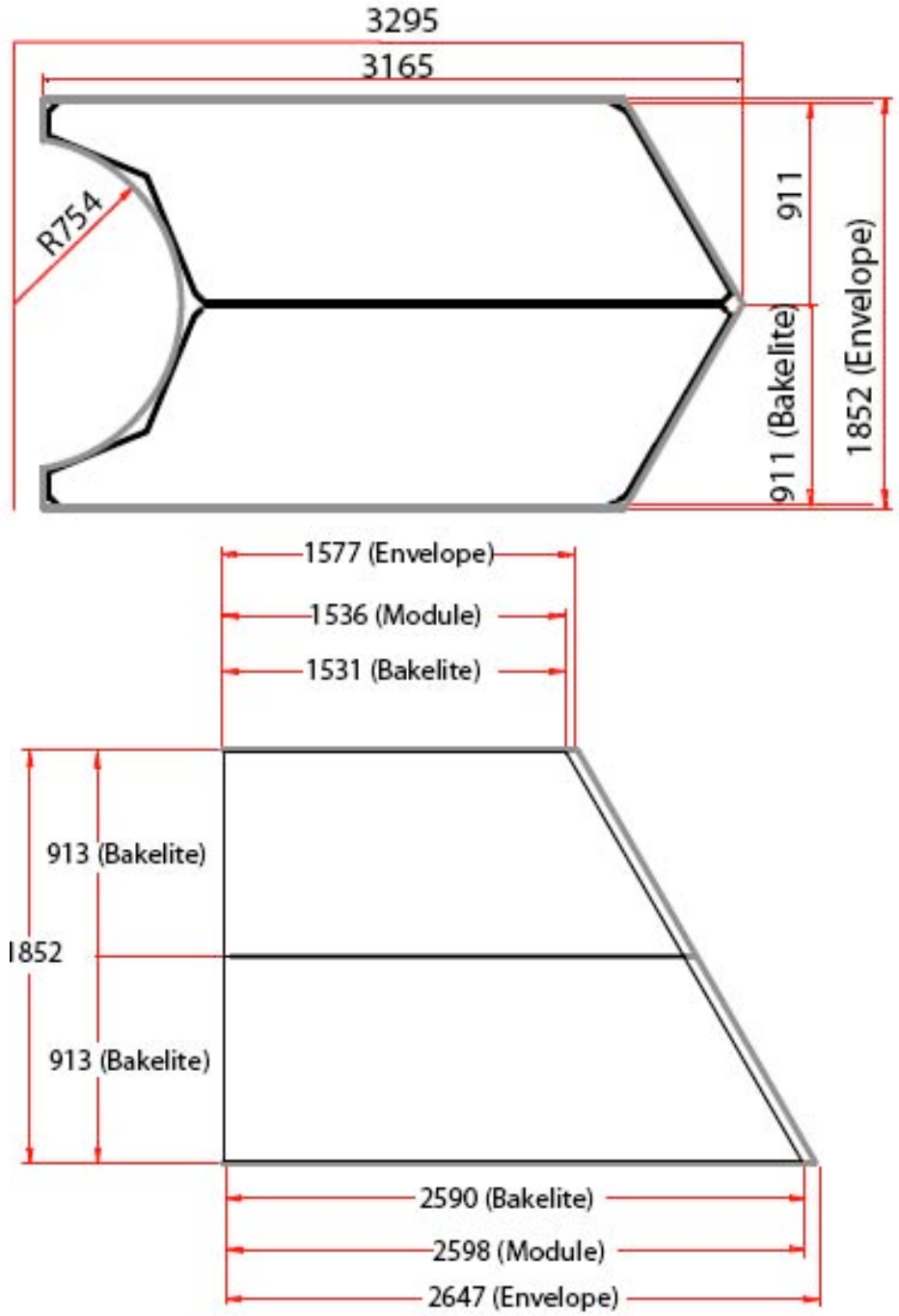

Fig. 8. Top: shape of a middle chamber. Bottom: shape of a top/bottom chamber

- Drill gas inlets and seal chamber.
- Coat the inner surfaces with linseed oil.
- Apply pickup strips and assemble HV modules into chambers.

Changes and improvements on all the items mentioned above were introduced for the new BaBar production. Some of the changes, such as improved graphite layers, were developed by LHC groups [7]. The difference mostly consists in a much finer graphite powder. Others were introduced during the BaBar production and were also adopted for the mass production of RPC chambers for the LHC experiments. The most important changes, the introduction of corner pieces containing the gas inlets and changes in the oiling procedure are discussed in separate sections below. Other relevant changes are:

- Strict quality control on the bakelite surface finish (absence of scratches, bubbles and other defects) and cleanness.
- Lexan button spacers were cleaned by an ultrasound washing machine.
- The bakelite sheets were cut to shape using milling machines instead of by sawing ensuring a more precise and cleaner edge which made the mechanical coupling among the bakelite slabs, frames and corner pieces easier.
- Major improvements in the cleanliness of the production area were implemented by the factory.
- New tools for handling of the bakelite slabs during the assembly were introduced to avoid contamination of the surfaces by contact with hands and to ensure better precision in the positioning of the top slab.
- Particular care was required in checking and cleaning the slab immediately prior to gluing.
- The gluing process has been automated on regular shapes (Belt chambers) with an automated gluing machine. However, all the BaBar forward endcap RPCs were glued with the old manual technique. Glue samples (spacers on small bakelite squares) were prepared every day to check for proper glue curing before moving the assembled gap.
- The hot melt (used for sealing the chambers along the edges) dispenser was improved.
- Mechanical stresses in the final assembly of the chambers were minimized by the introduction of special trays on which the chambers rode during handling, testing and most important, shipping.

3.2 Inner linseed oil surface

A thick and uncured linseed oil film on the inner surface of the detector was the most evident source of malfunctioning RPCs in BaBar. For the new production we chose to have a thinner film by changing the fraction of eptane in the oil mixture from 70:30 (linseed oil:eptane) to 40:60 and by using a single fill of

the gas volume (instead of three). A thinner film, however, makes the chamber more sensitive to dust and particulate that exceed the paint thickness (10-30 μm).

As stated before, this requires elimination or reduction of every possible source of contaminants in every phase of the construction process. The global area cleanness, the visual inspection and cleaning of the slabs before assembling, the introduction of filters both in the oil and air circuit for the inner surface painting, and most importantly, the introduction of the gas inlet corner pieces, were all taken to greatly reduce such effects. Quality controls on the inner surface painting included: chemical analysis of the linseed oil mixture in every oiling cycle as well as visual inspection and chemical analysis of the cured inner surfaces of a sacrificial chamber from each oiling group.

3.2.1 New linseed oil coating procedure

The inner coating was done by completely filling the gas volumes with linseed oil. The chambers were tightly packed vertically in groups of 12-20 pieces to compensate for mechanical stresses due to the rising oil pressure. The filling was aided by gravity. A 250 liter tank containing the oil mixture was slowly raised above the top of the chambers (Fig. 9).

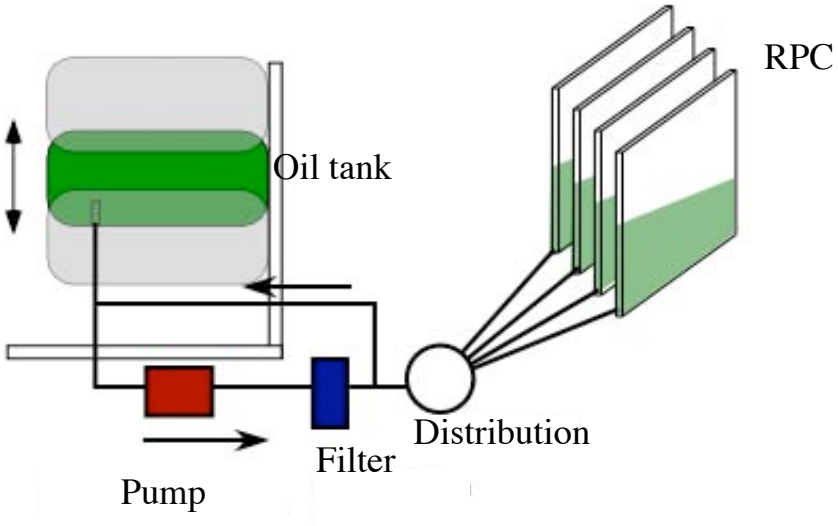

Fig. 9. The new oiling set-up with Nylon filter and pump.

After filling, the chambers were emptied by slowly lowering the tank in $\simeq 3$ hours. The oil draining from the chambers potentially carried dust or other

particles back into the tank. To avoid contaminating the next oiling step the oil circuit was modified to include a 5μm Nylon filter that was chemically compatible with eptane. To force the oil through the filter, a gear pump with magnetic drive and a steel head was installed. Again the material and technology of the pump was chosen to be compatible with eptane to avoid chemical contamination. The complete polymerization of the oil film was achieved by flushing the chambers with air for 36 hours in a temperature controlled environment (40 ^0C). The air circuit was equipped with a paper filter to get rid of dust at the 5μm level. Density measurements every two oiling cycles ensured the proper composition of the mixture.

3.2.2 Chemical analysis

Chemical analysis QA procedures covered each of the painting steps by analyzing samples of:

- Fresh linseed oil.
- Linseed oil and eptane mixture.
- Mixture after oiling every group.
- Polymerized oil on the surface of a sacrificial chamber, which was chosen randomly from each oiled group and opened to inspect the inner surfaces .

The analysis was performed using the FTIR (Fourier Transform Infrared Spectroscopy) technique which looks at the vibrational spectra of the molecules in the sample, allowing the identification of different kinds of bonds and compounds. With FTIR one can tell whether the oil is fully polymerized or if the oil has degraded as indicated by the presence of free fatty acids. It can also identify the presence of contaminants (such as phthalates) which might prevent the proper curing of the oil. No structural differences are visible in Fig. 10 in the FTIR spectra of surfaces painted with a fresh linseed oil/eptane mixture and a chamber from the production cycle. In both cases the oil was completely polymerized. No contaminants were ever detected during or after construction.

3.3 Gas inlet/corner pieces

As described in a previous section some of the new style RPCs installed in year 2000 with thinner linseed oil layers developed areas of high noise rates and lowered efficiency near the gas inlets. Debris in this area appeared to be the residual of the drilling of a completed chamber to insert the gas inlet/outlet pipes. Although a vacuum tool was used to minimize the amount of debris left inside the gas volume, some material was always trapped inside.

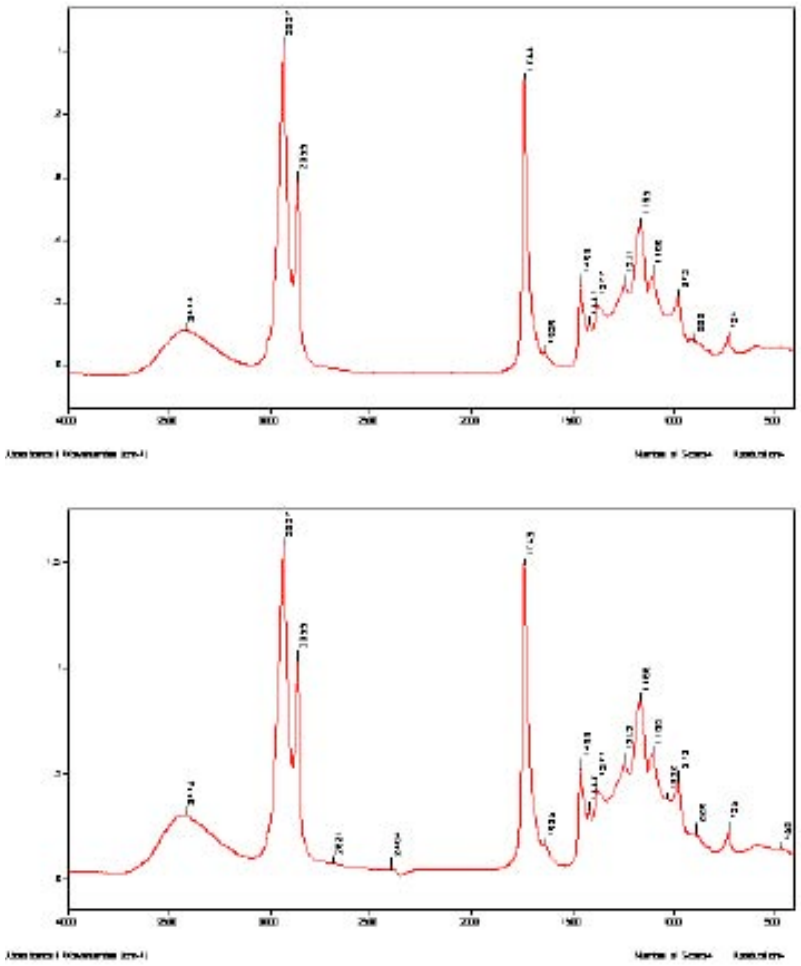

Fig. 10. The FTIR response for a fresh sample of linseed oil (upper) and a sample taken at at the output of the chamber oiling circuit

BaBar was the first experiment to introduce a new approach to this problem. The gas inlets were integrated into special frame pieces (corner pieces) which were mounted, with spacers and standard frame pieces, at the gas volume assembly stage. The main advantage of this approach was to avoid machining the sealed gas volume. The cleanliness of the volume was therefore set by the surface quality of the slabs before chamber assembly. This procedure made the assembly more complicated and reduced the inner diameter of the gas fitting from 3.0 to 1.5 mm. The picture (Fig. 11) shows a section of the gas volume with the corner piece inserted. The introduction of the T shaped corner pieces

constrained the alignment of the bakelite and frame pieces. In previous RPC productions the bakelite slabs were cut to $\approx \pm 2$ mm by saw. Depending on the length difference among the top and bottom slabs it was possible for the slabs to slide over the edge of the corner piece when the vacuum press was applied. Improving the precision of the slab cutting by use of a milling machine solved the problem.

Fig. 11. Picture of the corner piece in place

4 Quality Control and results

Many of the quality control procedures introduced in the new RPC production were performed by factory technicians and were logged onto QC forms covering each step of the production chain. The QC data were typed daily into the production database by BaBar personnel.

4.1 QC forms

The QC forms covered:

Preparation of the raw material

- Bakelite surface quality
- Graphite painting quality and resistivity (by sample)
- PET gluing

Gap assembly

- Glue samples
- Temperature and humidity check

Oiling

- Fresh Linseed oil sample chemical analysis
- Eptane linseed oil mixture chemical analysis (every oiling cycle)
- Mixture composition (every two oiling cycle)
- Sacrificial chamber inspection (every oiling cycle)
- Gas volume oiling history

4.2 Test on assembled chambers

In addition to the QC controls done by factory personnel to certify that the gas volumes were produced strictly to our technical specifications, checks were made by BaBar personnel at the factory on the completed gas volumes and assembled chambers. The gas volume tests searched for mechanical or electrical defects, undetected during construction, which could affect performance before these gas volumes were used in the final chamber assembly. The final test used cosmic rays in a test stand with standard BaBar-like running conditions (gas mixture and HV distribution).

4.2.1 Leakage and push tests

BaBar RPCs are bare, without an external mechanical frame or support as used by other experiments to avoid mechanical stresses on the spacers and frames. For example flushing the chamber with an overpressure of 10 millibars applies a force of 10 x 100 g on each spacer (the buttons are set on a 10 x 10 cm^2 grid). Spacers unglued or poorly glued can detach under small overpressure. The nominal strength of the two component glue used in the construction is 40 kg per spacer. Detached spacers allow local deformations of the bakelite, even under small overpressure, which increase the gap between the bakelite high voltage surfaces. This could reduce the electric field below the value needed to produce streamers in the RPC gas, reducing the efficiency in the area near the button. The presence of poorly glued spacers could be the result of many different problems in the production chain. Possible sources are poor bakelite surface or spacer cleanliness, strange bakelite surface textures or bad glue curing.

To detect gas leakage or popped buttons a simple tool based on a pressure sensor and a few brass weights was developed. A low pressure sensor (0-7 mbar) was read out by a 16 bit sampling ADC board using a PC running a Lab View program [1] to provide a real time display of pressure versus time (Fig. 12).

A single popped button could induce a pressure variation of several percent when the chambers were first pressurized. The gas pressure measurements were sensitive to a tenth of a percent. Gas leaks were detected by raising the pressure inside the gas volume to 6 mbar, closing the inlet valve, and looking for pressure variations with time. Temperature was also monitored as the system was quite sensitive to small temperature variations during the test (easily caused by small changes in the intensity of the ambient sunlight on the black RPC surface). Popped buttons were detected with even greater

[1] Lab View is a Trademark of National Instruments.

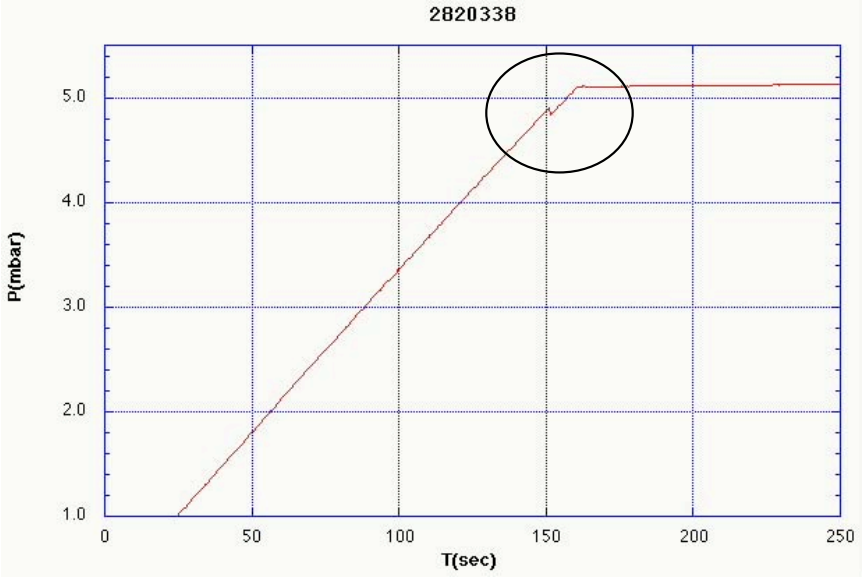

Fig. 12. The little kink (circled) near the knee signals a spacer popped by the rising pressure.

sensitivity by placing a bar equipped with twelve floating weights (push test) over a row of buttons with the chamber still at 6 mbar internal pressure. Each weight was placed over a corresponding button (see Fig. 13). The brass weights were 600 g each thus balancing the internal pressure. If all the spacers in the row under test were glued, the brass weights pushing on the spacers did not induce a pressure change in the system. If one or more buttons were popped, the effect of the weight was to restore the normal distance between the bakelite slabs, decreasing the gas volume and raising the internal pressure. Fig. 13 shows the result of a push test on 19 rows of buttons in the gas volume. Each step corresponded to a push on a specific spacer row. The pressure was nearly the same in every row except for row 13 where a clear increase was observed, indicating one or more popped buttons in this row.

To identify which buttons were popped, the bar was put back in place over the suspect row and the weights were raised and lowered one by one. When the weight over a glued button was raised no significant pressure change was seen. When the weight over a popped spacer was raised the volume of the RPC increased and a pressure decrease was observed.

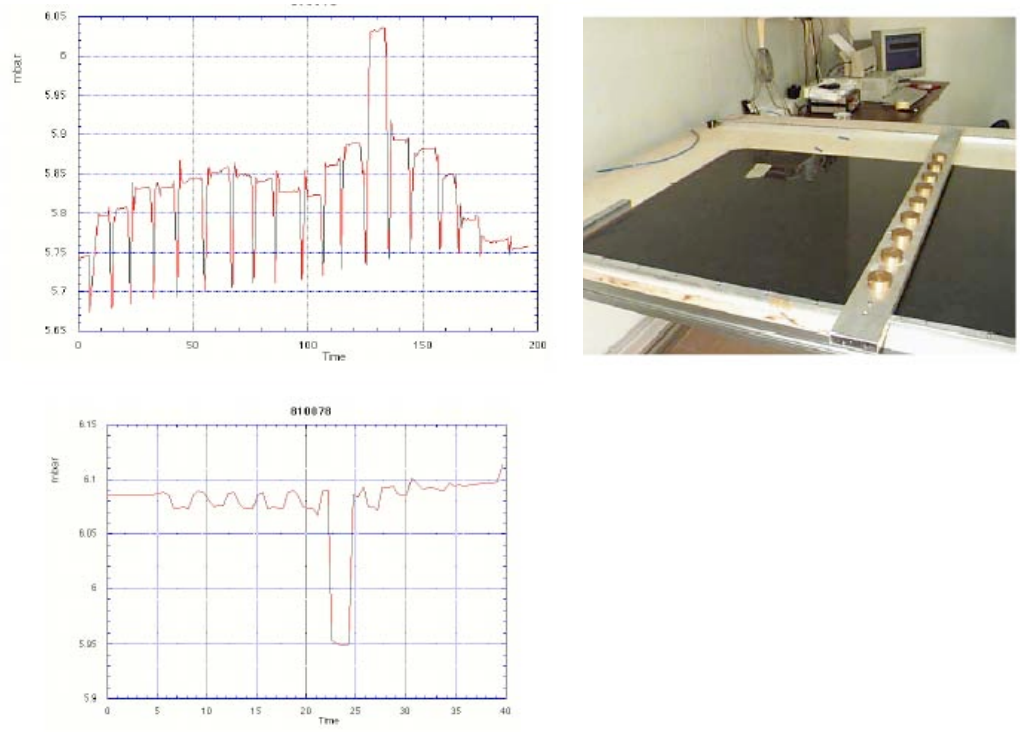

Fig. 13. Top-Left: result of the push test on all the 19 spacer lines. Bottom-Left: evidence of an unglued spacer on line 13. Right: the push test set-up

4.2.2 Current vs. HV test

After the push test each gas volume was flushed with the standard BaBar gas mixture for 24 hours and the characteristic current vs. voltage curve was measured. Good gaps show a negligible linear Ohmic contribution up to the threshold for discharges in the gas which occurs around 5.5 kV. The current then grows exponentially. The test measured the current up to 7kV where the streamer regime is expected to be fully efficient (Fig. 14).

The gas volume was accepted if the current at 7kV was below $2\mu A$.

Several chambers had a non-negligible linear raise during the initial turn on. Fig. 14 shows one of these situations (dark dots). The current normally drops to lower values after a short conditioning cycle done by raising and lowering the voltage from 0 to 8 kV. The Ohmic contributions never disappear completely. Chambers were considered good and the conditioning successful if the current at 5.5 kVolt was below 1 μA.

The conditioning cycle had no significant effect on good chambers.

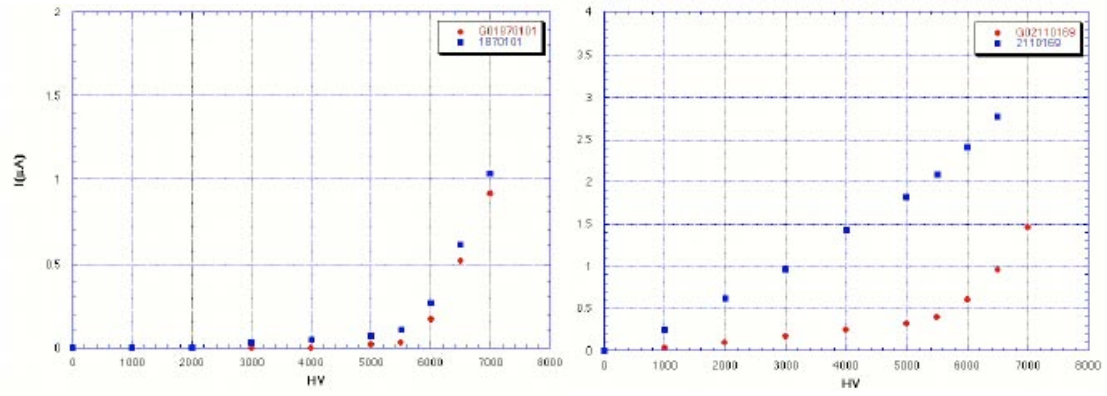

Fig. 14. Left: I vs. HV characteristic curve for the same chamber measured before (squares) and after (dots) conditioning. The typical current at 7 kV is less than $2\mu A$. Right: The same curve for a chamber that needed conditioning.

4.2.3 Plateau and radiographies

Successful completion of all the pre-production tests (leak test, push test and I/V curve) were pre-requisites for assembling pairs of gas volumes into one endcap chamber. Two electrode sheets were glued on both sides of the gas volumes, so as to form a grid with "vertical" strips (we refer here to the final orientation when installed in the experiment) on one side and "horizontal" on the other one. Up to 12 chambers were stacked on aluminum trays, 2m wide by 3m long, assembled expressly for this test. The trays in this "tower" had handles allowing them to be safely removed and stacked more closely in another structure used for the shipping; in this way, each finished chamber was subjected to the minimum mechanical stress. After a first rough alignment of chambers, that brought all offsets of strip layers to zero within 5-10 mm, the 24 strip systems of a "cosmic stack" were connected to the same readout electronics used in the real experiment. HV connections were made to a distribution box of the same type employed in the new BaBar installation, allowing currents and voltages to be continuously monitored through a CAN-BUS system. A gas system flowing up to 12 circuits in parallel was employed: each individual circuit was controlled by a gas flowmeter. Both the rates of gas flowing into and from the chambers were measured by 2 displays for each circuit. The equality of the readouts (as well as a preliminary check using common bubblers) assured the tightness of all gas connections and chamber integrity.

The top and bottom chambers remained in place throughout the period of construction, and generated the trigger for the DAQ: signals from the FAS-

TOR of the 16 strips connected to each electronic card were ORed within each trigger layer and ANDed between the top and bottom chamber. This logic signal was sent to a custom trigger module housed in a VME crate. A PC running a LabView program was used to sense the hardware trigger, and read out the system via a custom made readout module. The data (the pattern of hit strips) were written to disk and subsequently moved to a second PC through a small LAN for immediate analysis.

The data collected with the cosmic ray test stand has been analyzed off-line. The data was first unpacked into a list of hit strips, then adjacent hit strips were joined into clusters to account for possible > 1 multiplicity. The center of each cluster gave the coordinate of the impact point of the cosmic ray in each of the two orthogonal projections.

The passage of a real cosmic ray through the chambers under test was established in hardware by the coincidence of the signals from the trigger chambers positioned in the highest and lowest layers of the test setup. In software, it was then required that there be one and only one cluster in each of these trigger chambers. The straight line connecting the two clusters in each orthogonal projection was then used to define a cosmic ray track, whose impact point on each of the test chambers was taken as that chamber's expected hit position.

A residual was then calculated as the difference between the expected coordinate and the coordinate of the cluster closest to it. We defined the efficiency of a given chamber to be the ratio of the number of tracks crossing it divided by the number of times a cluster actually measured in both projection (AND of the two views) had its coordinate laying within 6 cm in X (corresponding to $\sim 3\sigma$) and 9 cm in Y ($\sim 3\sigma$) from its expected position. Fig. 15 shows the distribution of the residuals for one of the chambers.

We could in this way obtain both one-dimensional projections of the efficiency as a function of the horizontal or vertical coordinates, and 2D maps of the efficiency as a function of both (radiographies).

After inserting the chambers into the test stand and completing all the cabling, a first run of about 100k events was taken to establish the integrity of the data itself, check cabling and mapping between the hardware and software channels. Then a high statistic sample ($\sim 10^6$ events) was taken at the nominal working HV of 7.4 kV, which we used to perform a high resolution radiography of every single chamber.

A series of lower statistics runs taken at increasing high voltage setting was then taken to perform an efficiency plateau for every single RPC (each chamber was made of two individual RPC side by side held together by the common strip planes). In Fig. 16 we show an example of the plateau curve for the two RPCs in a chamber.

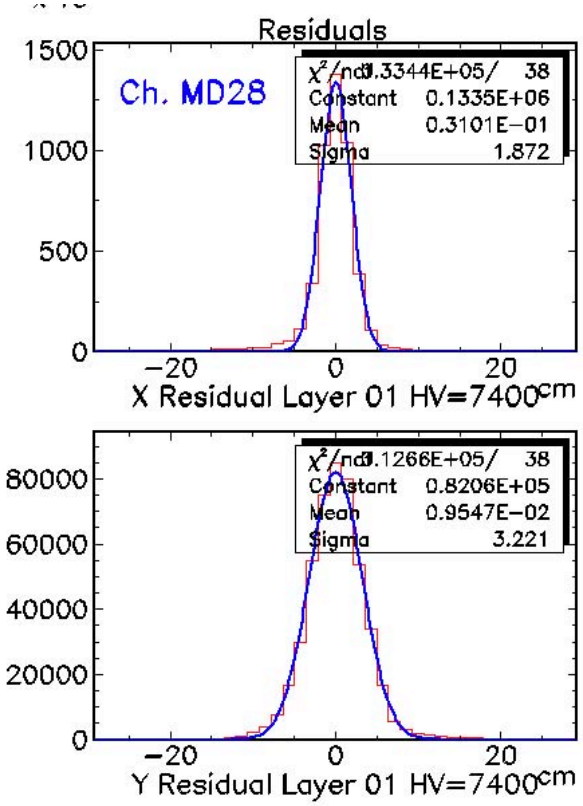

Fig. 15. A typical distribution of the residuals. Top plot: x coordinate, Bottom plot: Y coordinate

Together with the efficiency and plateaux, many other quantities were plotted and stored with the construction record of each chamber, like the strip occupancies and residual as a function of X and Y coordinates.

Despite its name, the offline analysis was performed almost online, as it occurred right after the data was taken. Moreover, as it was performed at the factory, immediate feedback to the operators doing the construction was possible. On a few occasions chambers were sent back for minor repairs (mostly disconnected strips due to a bad soldering).

Almost all the chambers had no detectable defects. On only one occasion did a relatively severe defect (a few unglued spacer buttons) show up in a radiography. In Fig. 17 we show the radiographies for both a good chamber

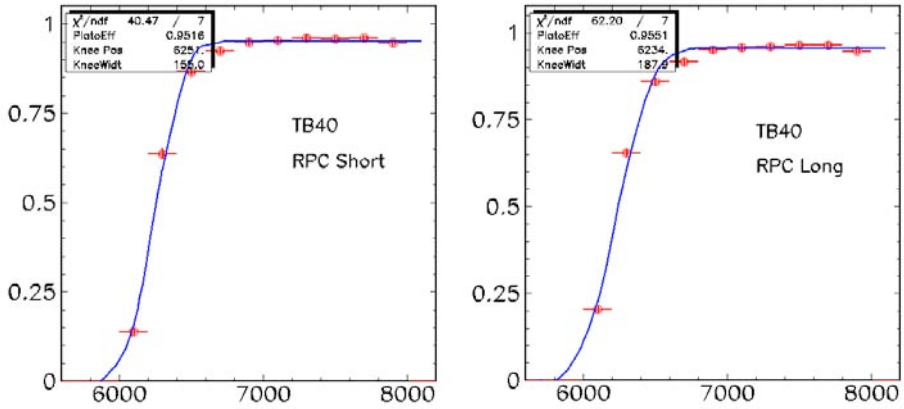

Fig. 16. An example of the plateau curves for the two RPC modules that form a chamber.

and a chamber with popped buttons. The radiography for the faulty chamber in the figure was taken while flushing the chamber with gas at high flow rate (therefore inducing an overpressure much higher than expected during normal running).

Subsequent radiographies taken at lower flux (overpressure) showed a dramatic lowering of the effect. This kind of problem is greatly mitigated, if not totally eliminated, by the mechanical constraints to which the chambers are subject when inserted in the final apparatus, which tend to push the two plates together.

We have assembled about 125 chambers. The 25 belt chambers are single gap, single module while the rest are single gap, double module. Thanks to the QC program we have been able to reject before actually assembling the final chambers on the order of 30 gaps. Eighteen of them have been discarded because they did not pass the push/leak test; 8 because they could not be HV conditioned and 4 that we had to sacrifice for visual inspection. The other sacrificial chambers were chosen amongst the ones already rejected for other reasons. The push/leak test allowed the discovery that some of the bakelite was of a different nature than previous samples and did not adhere properly to the spacers. Most of the 18 modules rejected for this reason were of the belt type. No fully assembled chamber was ever rejected.

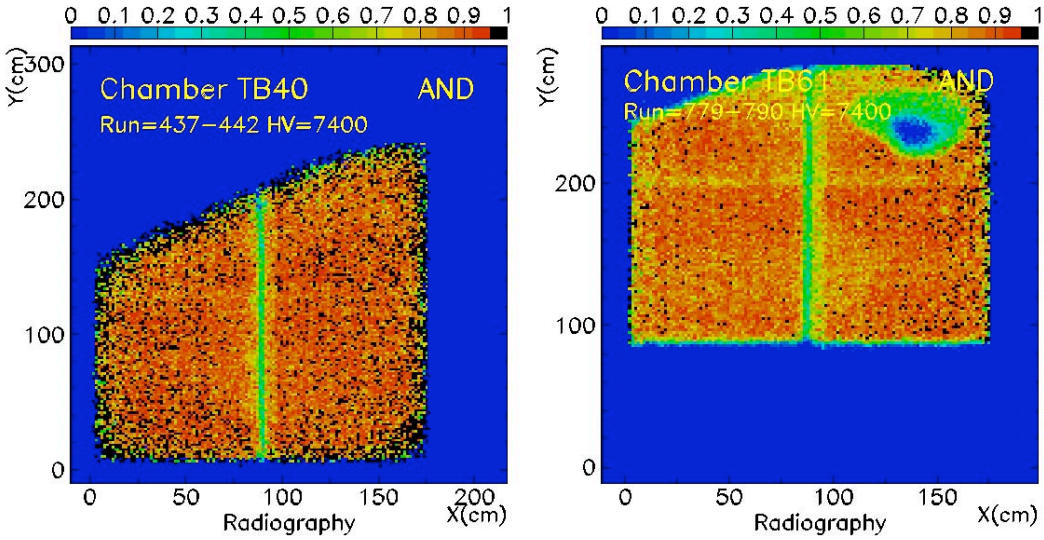

Fig. 17. The radiographies for both a good chamber (left) and the chamber with the popped buttons (right).

5 Detector Installation

5.1 Transport and storage

RPCs were shipped in wooden boxes to SLAC, each box containing typically 12 chambers. The chambers were housed horizontally on trays to avoid any stress during transport. In the subsequent operations prior to installation, the chambers were always kept horizontal, each chamber on its own tray. Up to 12 trays were stacked in a metal structure mounted on wheels so as to be movable smoothly without stressing the chambers.

5.2 QC at SLAC

Each RPC was tested again for gas tightness and efficiency upon its arrival at SLAC. A cosmic test stand was created to closely match the BaBar detector configuration as far as the gas distribution, high voltage, and layer spacing were concerned. Premixed standard BaBar RPC gas was used. Chambers were tested at nine voltage settings between 5500 and 7400 V. At each setting, measurements were performed of the average efficiency and cluster size. A

high statistics 2D efficiency map was made at each voltage setting to check the uniformity of the response. Chambers were accepted for installation if they were found to be gas tight and had an efficiency $> 90\%$ at 6800 V. Essentially all chambers passed these criteria. The minor defects found at this stage were mainly broken gas inlets which were promptly fixed.

5.3 Chamber Dressing

Upon completion of the efficiency measurements the chambers were assigned to specific locations in the detector and the final labels applied. In addition the cables were taped down and routed to specified positions on the edge of the chamber to make the cable hook-up after installation easier. An aluminum channel was added to the bottom edge of the chamber for protection and to aid installation. The channel was slightly longer than the RPC and contained a screw which could be grabbed if the chamber had to be removed.

5.4 Installation into BaBar

For the installation, dedicated mechanical fixtures developed for the previous installation in 2000 were used. The procedure was to take the chamber on its tray out of the scaffold , to slide it gently into the fixture horizontally and to rotate the fixture vertically with a crane. Careful attention was paid in order to avoid any twisting of the chamber or cables and gas hoses. After crane transport, the chamber was pushed slowly into the appropriate slot by pushing the reinforcing channel, not the chamber itself. Installation into the endcap doors lasted from August 14th until September 20th as scheduled. On average, three hours were needed to install 12 chambers. HV and leakage tests were done immediately after insertion. Only one chamber was removed and reinstalled to repair a broken gas inlet.

6 Conclusions

In this paper we have illustrated the need for rebuilding the muon and neutral hadron identification system of the BaBar collaboration. From the experience with the original detector we were able to redesign the detector geometry to improve the muon identification performance by altering the absorber to active layer ratio. After an extensive study of the possible RPC failure modes we made many changes to the manufacturing procedure with an emphasis on detector cleanliness. A protocol for Quality Control and Assurance was

developed and strictly followed. The performance of all accepted chambers has been good in the year and half since installation and will be described in a forthcoming paper. We would like to remark that most of the procedures and protocols developed by BaBar for producing RPCs are routinely used by LHC experiments now building their counters at General Tecnica.

References

[1] B. Aubert et al., Nucl. Instr. and Meth. A 479 (2002) 1.

[2] R. Santonico and R. Cardarelli, Nucl. Inst and Meth. A 187 (1981) 377.

[3] General Tecnica S. r. l., I-03030 Colli (FR), Italy.

[4] H.R. Band, "Experience with the BaBar Resistive Plate Chambers" to be published in IEEE NSS-MIC 2003 Conference Record

[5] F. Anulli et al., Nucl. Inst and Meth. A 508 (2003) 128; F. Anulli et al., Nucl. Inst and Meth. A 494 (2002) 455; J. Va'vra, "Attempt to correlate the ionic model with observations in BaBar RPC chambers and R&D tests", Submitted to IEEE Trans. Nucl. Sci., 2003.

[6] C. Cartaro, F. Fabozzi and L. Lista, BaBar Note 540, Dec. 2001(unpublished).

[7] G. Aielli et al., Nucl. Inst. and Meth. A 515 (2003) 335.

[8] F. Forti and M. Lazzari, Linseed Oil Chemical analysis, Results presented at IFR Review, April, 2001. Stanford Linear Accelerator Center (unpublished).

[9] J. Va'vra, Nucl. Inst and Meth. A 515 (2003) 1.